

## Excitons in electrostatic traps

A. T. Hammack,<sup>a)</sup> N. A. Gippius,<sup>b)</sup> Sen Yang, G. O. Andreev, and L. V. Butov  
*Department of Physics, University of California at San Diego, La Jolla, California 92093-0319*

M. Hanson and A. C. Gossard

*Materials Department, University of California at Santa Barbara, Santa Barbara, California 93106-5050*

(Received 4 April 2005; accepted 7 February 2006; published online 21 March 2006)

We consider in-plane electrostatic traps for indirect excitons in coupled quantum wells, where the traps are formed by a laterally modulated gate voltage. An intrinsic obstacle for exciton confinement in electrostatic traps is an in-plane electric field that can lead to exciton dissociation. We propose a design to suppress the in-plane electric field and, at the same time, to effectively confine excitons in the electrostatic traps. We present calculations for various classes of electrostatic traps and experimental proof of principle for trapping of indirect excitons in electrostatic traps. © 2006 American Institute of Physics. [DOI: 10.1063/1.2181276]

A possibility of exciton confinement and manipulation in potential traps has attracted considerable interest. Excitons are bosonic particles in semiconductors, and studies of the bosons in controlled potential reliefs are of fundamental interest. In particular, confinement of bosonic atoms in traps is crucial for experimental implementation of atomic Bose-Einstein condensates.<sup>1,2</sup> Also, controlling the optical properties of semiconductors by manipulating the excitons in microdevices may be used to develop optoelectronic devices.

Pioneered by the electron-hole liquid confinement in the strain-induced traps,<sup>3</sup> exciton confinement has been implemented in various traps: strain-induced traps,<sup>4-6</sup> traps created by laser-induced local interdiffusion,<sup>7</sup> magnetic traps,<sup>8</sup> and electrostatic traps.<sup>9-11</sup> An advantage of the electrostatic traps is a possibility for creating a variety of in-plane potential reliefs with the required parameters for the excitons and a possibility for manipulating the relief *in situ*, thus controlling the optical properties both in space and in time. In particular, electrostatically induced transport of excitons<sup>12</sup> and the electrostatically controlled capture and release of photonic images<sup>11</sup> have been demonstrated.

The principle of the electrostatic traps is based on the quantum confined Stark effect:<sup>13</sup> An electric field  $F_z$  perpendicular to the quantum well (QW) plane results in the exciton energy shift  $\delta E = eF_z d$ , where  $d$  is the exciton dipole moment. For indirect excitons in coupled quantum wells<sup>10,12</sup> (CQWs), electrons and holes are separated in different QWs and  $d \approx L_{\text{QW}}$ , the distance between the QW centers. The laterally modulated gate voltage  $V_g(x, y)$  creates a laterally modulated electric field and, in turn, a lateral relief of the exciton energy  $\delta E(x, y) = eF_z(x, y)d$ . Control of  $V_g(x, y)$  allows manipulation of the in-plane potential profile for excitons both in space and in time. However, an intrinsic obstacle for exciton confinement in the electrostatic traps is an in-plane electric field  $F_r$  that can lead to exciton dissociation.<sup>13</sup> A strong exciton confinement in the electrostatic traps requires a strong lateral modulation of  $V_g$ , which can lead to a

strong  $F_r$  and exciton ionization.<sup>9</sup> In Ref. 9, the intensity of the exciton photoluminescence (PL) was decreased with increasing modulation of  $V_g$ , indicating that exciton ionization worked effectively against the exciton confinement to the electrostatic traps.

We modeled electrostatic trap geometries that are variations on the theme of a CQW in an insulating layer sandwiched between a patterned set of top gate electrodes and a single homogeneous bottom gate electrode. To find the field distribution for given voltages at the gate electrodes, the Poisson equation was solved numerically for a static dielectric constant using the boundary element method.<sup>14</sup>

The first trap is studied for AlAs/GaAs CQWs. It is obtained by making a circular hole in the top gate (Fig. 1). The separation between the gates is taken to be  $D = 1000$  nm, and the exciton dipole moment in AlAs/GaAs CQWs is  $d \sim 3.5$  nm. Figure 1(a) displays the calculated effective exciton potential  $\delta E(r) = eF_z(r)d$  for a top gate voltage of 1 V for two positions of the CQW—100 and 500 nm above the bottom gate. Note that a large distance from the QW to the bottom electrode  $zD = 100$  nm ensures high quality of the QW. This trap has only two gates and its spacial profile is controlled by the ratio of the hole diameter versus gate separation. The applied voltage modifies only the strength of the trap (at positive  $V_g$ ) or bump (at negative  $V_g$ ), not its shape.

The lateral component of the electric field  $F_r(r)$  at the CQW plane is shown in Fig. 1(b). Positioning the CQW close to the lower gate results in a strong suppression of the in-plane electric field at the CQW plane, by an order of magnitude for the example shown in Fig. 1. This is because the in-plane electric field is concentrated near gate edges and vanishes at the homogeneous bottom gate. The exciton ionization time reduces exponentially with the in-plane electric field  $\tau \sim \exp[4E_{\text{ex}}/(3eF_r a_{\text{ex}})]$ , where  $E_{\text{ex}}$  is the exciton binding energy and  $a_{\text{ex}}$  is the exciton Bohr radius [see Eqs. A6 and A7 in Ref. 13 for two-dimensional (2D) and three-dimensional (3D) excitons]. If the CQW is equidistant between the gates, the lateral electric fields reach  $0.2$  V/ $\mu\text{m}$  [Fig. 1(b)], and the estimated exciton ionization time [using Eq. A6 in Ref. 13] is in the picosecond range and exciton

<sup>a)</sup>Electronic mail: ahammack@physics.ucsd.edu

<sup>b)</sup>On leave from the General Physics Institute RAS, Vavilova 38, Moscow 119991, Russia and Institute of Physical and Chemical Research (RIKEN), Wako 351-0198, Japan.

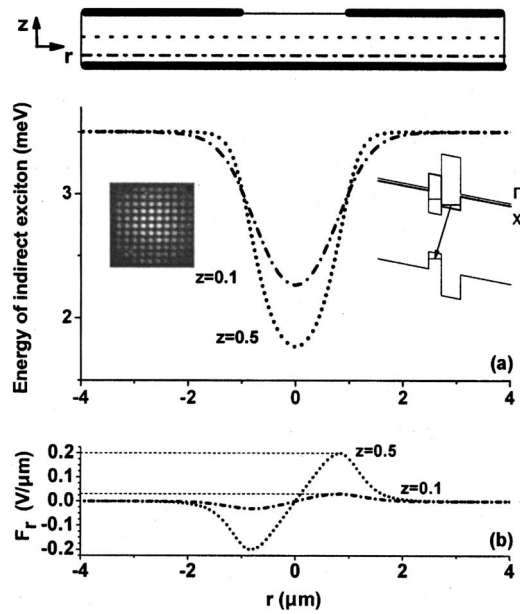


FIG. 1. Schematic cross section of an electrostatic trap formed by sandwiching an AlAs/GaAs CQW between a homogeneous bottom gate and a top gate with a hole. The indirect exciton effective potential (a) and lateral component of electric field in the CQW plane (b) are shown for  $V_g = 1$  V,  $D = 1000$  nm,  $d = 3.5$  nm, and for two CQW positions— $D_b = 100$  nm ( $z = D_b/D = 0.1$ ) and  $500$  nm ( $z = 0.5$ ) above the bottom gate. Left inset: The top gate electrode, which forms the periodic trap or bump arrays measured in the experiment. Right inset: AlAs/GaAs CQW band diagram.

ionization should be prominent. On the other hand, positioning the CQW at the  $1/10$  distance between the gates, closer to the homogeneous bottom gate, strongly increases the exciton ionization time (by 27 orders of magnitude according to the estimate using Eq. A6 in Ref. 13), thus making exciton ionization negligible. At the same time  $F_z$  is reduced only weakly and the exciton confinement potential remains strong [Fig. 1(a)].

This design can be employed for the creation of trap arrays or bump arrays with the modulation amplitude of the potential energy controlled by a single top gate with a periodic array of holes (Fig. 1). Note that the periodic trap array for excitons, where the modulation amplitude of the potential energy is controlled by a single top electrode, is similar to the optical lattice for atoms, where the modulation amplitude of the potential energy is controlled by the laser intensity.<sup>15</sup> The trap or bump arrays for excitons can be employed to study excitons in externally controlled potentials. Particularly interesting is the possibility to investigate the transition from delocalized to localized excitons (superfluid-insulator transition in the condensate case) with increasing amplitude of the potential, exciton temperature, or density.

The second type of trap is a multigated GaAs/AlGaAs CQW structure that allows elaborate control of the radial exciton potential profile [Fig. 2(a)]. The top gates comprise a system of ten  $200$  nm wide concentric rings with a ring width versus inter-ring separation ratio of  $2:7$ . The openings between the gates allow exciton photoexcitation over the entire trap area while the opening at the trap center allows optical signal collection for the exciton confined at the trap bottom (this is essential when nontransparent gates are used). An important example of potential trap profiles possible for

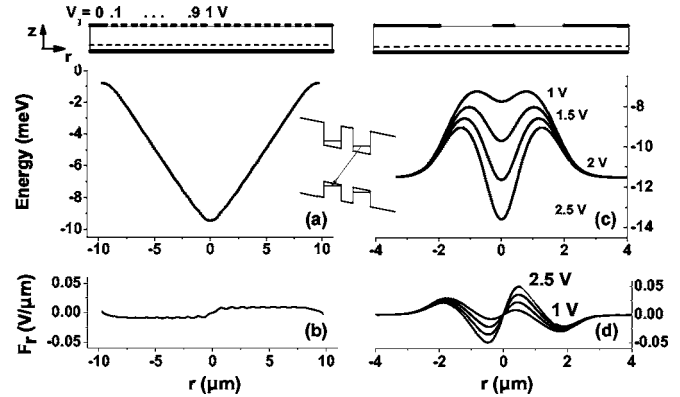


FIG. 2. The effective potentials and lateral electric fields for a conical trap formed by ten concentric rings with radially decreasing gate voltages  $V_g = 1-0$  V (a) and (b). A trap for evaporative cooling of excitons for  $V_g = 1$  V at external gate and  $V_{gc} = 1, 1.5, 2, 2.5$  V at center gate (c) and (d). Inset: GaAs/AlGaAs CQW band diagram.  $D = 1000$  nm,  $z = 0.1$ , and  $d = 12$  nm.

this geometry is a conical trap for the indirect excitons created by linearly increasing gate voltages toward the center of the structure [Fig. 2(a)]. The trap enables collection of a large number of excitons photoexcited over the entire large trap area at the trap bottom. The large exciton number at the trap bottom is essential for studies of exciton Bose-Einstein condensation (BEC) in traps since the critical temperature for BEC increases with the exciton density (for review of exciton condensation in confined systems see, e.g., Ref. 16). The gradual reduction of the gate voltage distributed over many gate electrodes allows keeping the in-plane electric field negligibly small [Fig. 2(b)], thus suppressing the exciton ionization.

The third trap type is designed for evaporative cooling of excitons. It has three gates: a bottom gate, an external top gate, and the central top gate [Fig. 2(c)]. For central gate voltages  $V_{gc} < 1$  V, the potential profile is a potential bump for the excitons. However, with the increase of  $V_{gc}$  a trap develops at the center of the bump that can be used for evaporative cooling of the indirect excitons. The most energetic excitons overpass the potential barrier and leave the trap, thus lowering the temperature of the exciton system in the trap. Evaporative cooling is effectively used for cooling atomic gases in traps.<sup>1,2</sup>

Following the computational modeling of the electrostatic exciton traps, we fabricated samples based on the first design type (Fig. 1). The studied electric field tunable  $n-i$  AlAs/GaAs CQW structure was grown by molecular beam epitaxy (MBE). The bottom  $n^+$  layer is Si-doped GaAs with  $N_{Si} = 2 \times 10^{18}$  cm<sup>-2</sup>. It serves as a homogeneous bottom gate. Unlike samples studied earlier,<sup>16</sup> a surface  $n^+$  layer was not grown for this sample to allow patterning the top gate by evaporated nontransparent metal contacts. The  $i$  region consists of a  $2.5$  nm GaAs layer and a  $4$  nm AlAs layer surrounded by two  $\text{Al}_{0.48}\text{Ga}_{0.52}\text{As}$  barrier layers with thicknesses of  $900$  and  $100$  nm for the upper and lower barriers. Mesas were etched and a patterned top metal electrode containing an array of circular holes with diameters of  $10$   $\mu\text{m}$  and periods of  $20$   $\mu\text{m}$  was deposited onto the mesas. A broad  $200$   $\mu\text{m}$  open area in the top electrode was fabricated as well for comparison. The sample was excited by a cw  $532$  nm

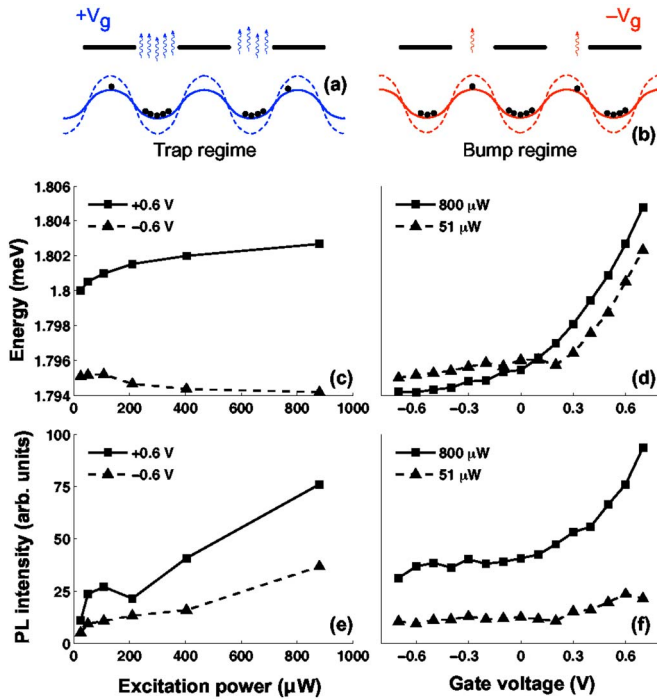


FIG. 3. (Color online) Experimental proof of principle for electrostatic trapping of excitons. Top panel: Scheme of the potential profiles for positive  $V_g$ , the trap regime (a) and negative  $V_g$ , the bump regime (b). The dependence of the PL line energy and intensity on laser excitation power at  $V_g=0.6$  and  $-0.6$  V (c) and (e). The dependence of the PL line energy and intensity on gate voltage for two excitation powers (d) and (f).

laser and the PL measurements were performed at  $T=1.6$  K.

First we note that essentially no change of the exciton energy versus gate voltage was detected in the  $200 \mu\text{m}$  open area. This indicates that consistent with our calculations an electric field is present in the CQW only in regions close to the upper gate.

The results for the indirect exciton PL for the array of  $10 \mu\text{m}$  holes as a function of gate voltage and excitation power are presented in Fig. 3. For the CQW type and contact geometry studied, positive applied top gate voltages should cause the formation of potential traps beneath the holes in the gate [Fig. 3(a)], while negative applied voltages should lead to potential bumps beneath the holes [Fig. 3(b)]. Figure 3(c) shows that increasing the exciton density leads to enhancement of the PL energy in the trap regime and its reduction in the bump regime. This corresponds to the expected behavior: The indirect excitons are oriented dipoles and interaction between them is repulsive.<sup>16</sup> The repulsive interaction leads to enhancement of the exciton energy in the area where the excitons accumulate and, in turn, to reduction of the exciton energy in between the areas of exciton accumulation<sup>17</sup>—the repulsively interacting excitons screen the external potential. In the trap regime, the excitons accumulate in the potential traps beneath the holes in the top gate [Fig. 3(a)] and the increasing exciton density in the traps is observed in the PL energy enhancement [Fig. 3(c)]. In contrast, in the bump regime, the excitons accumulate beneath the areas covered by the gates [Fig. 3(b)] and the increasing exciton density outside the holes in the top gate is observed in the PL energy reduction [Fig. 3(c)]. The exciton accumu-

lation in the traps beneath the holes in the top gate is revealed also by the stronger excitation power dependent intensity enhancement in the trap regime compared with that in the bump regime [Fig. 3(e)].

The transition from the enhancement of the PL energy with density to its reduction is observed around  $V_g=0$  V [Fig. 3(d)]. This is expected since the transition from the trap regime to the bump regime takes place at  $V_g=0$  V for the AlAs/GaAs CQWs. Finally, the formation of the electrostatic exciton traps by the laterally modulated gate voltage at positive  $V_g$  is accompanied by enhancement of the exciton PL energy and intensity [Figs. 3(d) and 3(f)] that is typical for the exciton accumulation in the traps. The observed enhancement of the exciton PL intensity and energy with the electrostatic trap formation shows that the exciton ionization due to the in-plane electric field is suppressed, and the excitons accumulate in the traps.

In conclusion, we proposed a design to suppress the in-plane electric field and at the same time to effectively confine excitons in the electrostatic traps. This is achieved by positioning the QW plane closer to the laterally homogeneous bottom gate and patterned top gate. Then, we presented calculations for various types of the electrostatic traps: traps for building the trap or bump arrays, traps for accumulation of a large exciton number, and traps allowing evaporative cooling for excitons. Finally, we presented experimental proof of principle for trapping of indirect excitons in electrostatic traps.

The authors are thankful to D. S. Chemla, T. Ishihara, L. S. Levitov, and S. G. Tikhodeev for useful discussions. One of the authors (N.A.G.) thanks Russian Federation for Basic Research and Russian Ministry of Science for partial financial support.

<sup>1</sup>E. A. Cornell and C. E. Wieman, *Rev. Mod. Phys.* **74**, 875 (2002).

<sup>2</sup>W. Ketterle, *Rev. Mod. Phys.* **74**, 1131 (2002).

<sup>3</sup>J. P. Wolfe, W. L. Hansen, E. E. Haller, R. S. Markiewicz, C. Kittel, and C. D. Jeffries, *Phys. Rev. Lett.* **34**, 1292 (1975).

<sup>4</sup>D. P. Trauernicht, A. Mysyrowicz, and J. P. Wolfe, *Phys. Rev. B* **28**, 3590 (1983).

<sup>5</sup>K. Kash, J. M. Worlock, M. D. Sturge, P. Grabbe, J. P. Harbison, A. Scherer, and P. S. D. Lin, *Appl. Phys. Lett.* **53**, 782 (1988).

<sup>6</sup>V. Negoita, D. W. Snoke, and K. Eberl, *Appl. Phys. Lett.* **75**, 2059 (1999).

<sup>7</sup>K. Brunner, U. Bockelmann, G. Abstreiter, M. Walther, G. Böhm, G. Tränkle, and G. Weimann, *Phys. Rev. Lett.* **69**, 3216 (1992).

<sup>8</sup>P. C. M. Christianen, F. Piazza, J. G. S. Lok, J. C. Maan, and W. van der Vleuten, *Physica B* **249**, 624 (1998).

<sup>9</sup>S. Zimmermann, A. O. Govorov, W. Hansen, J. P. Kotthaus, M. Bichler, and W. Wegscheider, *Phys. Rev. B* **56**, 13414 (1997).

<sup>10</sup>T. Huber, A. Zrenner, W. Wegscheider, and M. Bichler, *Phys. Status Solidi A* **166**, R5 (1998).

<sup>11</sup>J. Krauß, J. P. Kotthaus, A. Wixforth, M. Hanson, D. C. Driscoll, A. C. Gossard, D. Schuh, and M. Bichler, *Appl. Phys. Lett.* **85**, 5830 (2004).

<sup>12</sup>M. Hagn, A. Zrenner, G. Böhm, and G. Weimann, *Appl. Phys. Lett.* **67**, 232 (1995).

<sup>13</sup>D. A. B. Miller, D. S. Chemla, T. C. Damen, A. C. Gossard, W. Wiegmann, T. H. Wood, and C. A. Burrus, *Phys. Rev. B* **32**, 1043 (1985).

<sup>14</sup>G. Beer, *Programming the Boundary Element Method: An Introduction for Engineers* (Wiley, New York, 2001).

<sup>15</sup>M. Greiner, O. Mandel, T. Esslinger, T. W. Hansch, and I. Bloch, *Nature (London)* **415**, 39 (2002).

<sup>16</sup>L. V. Butov, *J. Phys.: Condens. Matter* **16**, R1577 (2004).

<sup>17</sup>A. I. Ivanov, *Europhys. Lett.* **59**, 586 (2002).

Copyright 2006 American Institute of Physics. This article may be downloaded for personal use only. Any other use requires prior permission of the author and the American Institute of Physics.

The following article appeared in J. Appl. Phys 99, 066104 and may be found at <http://link.aip.org/link/?JAPIAU/99/066104/1>.